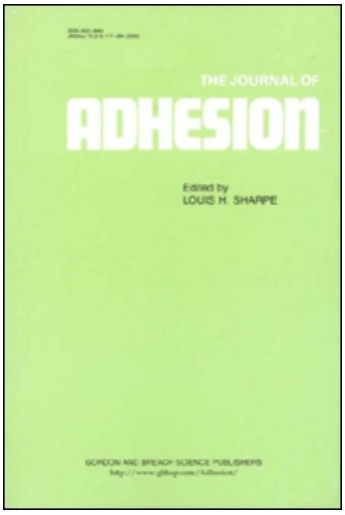

The Journal of Adhesion
Publication details, including instructions for authors and subscription information:
http://www.informaworld.com/smpp/title~content=t713453635

The Effect of Superimposed Dynamic and Static Stresses on the Stress Relaxation Rates of Model Epoxy Resins

S. Bron[ab]; D. Katz[a]
[a] Department of Materials Engineering, Technion-Israel Institute of Technology, Haifa, ISRAEL [b] Chemistry Department, Rutgers, The State University of New Jersey, Piscataway, NJ, USA

To cite this Article Bron, S. and Katz, D.(1993) 'The Effect of Superimposed Dynamic and Static Stresses on the Stress Relaxation Rates of Model Epoxy Resins', The Journal of Adhesion, 43: 1, 35 — 53
To link to this Article: DOI: 10.1080/00218469308026586
URL: http://dx.doi.org/10.1080/00218469308026586

J. Adhesion, 1993, Vol. 43, pp. 35–53
Reprints available directly from the publisher
Photocopying permitted by license only

Printed in the United States of America

The Effect of Superimposed Dynamic and Static Stresses on the Stress Relaxation Rates of Model Epoxy Resins

S. BRON* and D. KATZ

Department of Materials Engineering, Technion–Israel Institute of Technology, Haifa-32000, ISRAEL

(Received December 28, 1992; in final form May 21, 1993)

Model epoxy resins with controlled crosslinking densities were prepared from a commercially available DGEBA (Epon Resin 825® from Shell Chemical) and α,ω-aliphatic diamines having different lengths of the aliphatic chain. The mixtures were always prepared in stoichiometric ratio. Dumbbell specimens, either with a cylindrical (with thin walls) or a rectangular cross section, have been subjected to combined static tensile strains (applied vertically) and dynamic torsional strains (applied horizontally). The experiments were performed at temperatures encompassing the glassy and the rubbery range of each investigated resin. The apparatus, by which the combined dynamic and static stresses were applied, was equipped with load cells for measurement of stresses developed in the specimens, both in tension and in shear. In this paper, results concerning the effect of the above combinations of stresses on stress relaxation rates in tension are shown. The main conclusion of this study is that combinations of dynamic and static stresses affect the network chain mobility, as it is expressed by the stress relaxation rate, in a way depending on temperature and frequency of torsional oscillations, as well as the crosslinking density of the polymer. For the most flexible epoxy resins investigated in this work, the superimposed stressing experiments led to a stiffening of the structure in the glassy state, while an opposite effect has been observed for the most rigid resins in similar conditions. It seems that the behavior of the investigated epoxy resins in complex fields of stresses is governed by a balance between two competitive processes: free volume increase (by a strain-induced dilatation mechanism), and physical aging and short range orientation.

KEY WORDS combined dynamic and static stresses; stress relaxation rate in tension; crosslink density; model epoxy resins; free volume; physical aging; glass transition temperature; glassy state; rubbery state; strain-induced dilatation; rheological behavior; competitive processes; interphase.

INTRODUCTION

In previous papers,[1–4] the behavior of adhesive joints based on some epoxy adhesive formulations was described as a function of the resin composition and loading conditions. The most important conclusion was that combined dynamic and static stresses have a pronounced influence on the properties of the joint. The strength of Single

*Corresponding author. Present address: Rutgers, The State University of New Jersey, Chemistry Department, Busch Campus, Wright-Rieman Labs, Piscataway, NJ 08855-0939, USA.

Lap Joints increased as a result of application before testing of combined torsional oscillations and static shear creep at temperatures lower than the T_g of the adhesive; the opposite effect was observed with the same loading conditions in experiments performed above T_g.

To the best of our knowledge, the effect of superimposed dynamic and static stresses on polymers in their glassy state was not investigated before, and even for polymers in their rubbery state a very sparse literature exists on this subject. This is quite surprising in view of the fact that even combinations of different static stresses proved to have highly nonlinear effects on the properties of various polymers.[5–13] Findley and Onaran[13] defined effects observed in combined tension and torsion as "synergistic." Nishitani[10] stated that there is no possibility to predict the behavior of nitrocellulose in combined tension and hydrostatic pressure from experiments performed separately in each one of these loading modes, and Umanskii *et al.*[11] proposed a new standard test of adhesive joints in which shear and normal stresses can be simultaneously applied in various proportions by means of an original device. Most publications dealing with the application of combined dynamic and static stresses describe studies of the effect of static strains (or stresses) on some dynamic properties of polymers;[14–17] in these studies, the dynamic loads (or strains) were purposely very small, so that they should not affect the basic structure and the linear behavior of the polymer. Yet there are almost no publications dealing with the effect of combinations of finite dynamic and static strains on the properties and structure of solid polymers. Some studies were performed on polymer solutions subjected to combinations of steady shear and sinusoidal shear,[18–22] but we are aware of only one study[23,24] dealing with the mutual interrelation between finite static and dynamic strains applied on filled and unfilled rubber.

EXPERIMENTAL

The main objective of this study was to investigate the structure-property relationships of some epoxy resins as a function of crosslink density and loading parameters in complex fields of dynamic and static stresses.

Instrumentation

The static (tensile) and dynamic (torsion) loads were applied in controlled atmosphere in reciprocal perpendicular directions simultaneously on up to 5 bulk specimens, by means of a special apparatus, conceived and built for this research.[25–27] See Figure 1.

In most cases, the applied strain was about 1% in both modes of straining while the temperature was varied over a large range comprising the glass transition region of each one of the investigated resins ($T_g \pm 20$–$30°C$). The tensile strain was applied vertically by means of the special screw 11 (Fig. 1) which pulled down the crossheads 18 and 20. Their smooth and precise movement was performed along the columns 10, using 4 linear precision bearings. Dry nitrogen was supplied at about 1 l/min

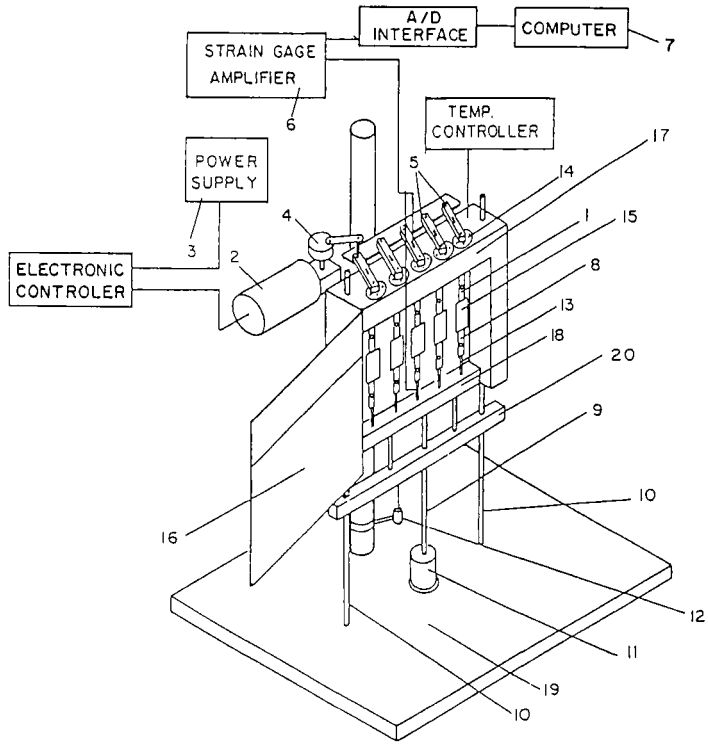

FIGURE 1 General picture of the experimental layout (see details in text).

per specimen. Each specimen's position was equipped with two load cells (13) for measurement of tensile and torsional stresses, respectively. The load cells were built as full Wheatstone bridges (nominal electrical resistance of 350 Ω) so that they had a temperature self-compensation, and were repeatedly calibrated by use of a dead-weight technique and calibration software written especially for this research. The torsional oscillations were applied at the upper end of the specimens through a complex mechanical system (5) activated by a frequency-controlled DC motor (2,3). The amplitude was changed by means of a variable eccentric (4). The temperature was controlled with the oven 16 and an Eurotherm temperature controller. The instrument has a compliance of about 0.0025 mm/kg, as measured using a high modulus steel specimen instead of regular specimens.[28] The stress was monitored by means of a computerized data acquisition system built purposely for this research. The signal generated by the load cells was fed into a strain-gage signal amplifier (6) and from there into an IBM-compatible computer (7) via a 16-channel A/D interface. A dedicated measurement program collected the incoming data in selected channels at predetermined sampling frequencies and recorded the digital signals in form of ASCII files on magnetic media. Usually, the sampling frequency was chosen so that at least 50 measurements were collected per specimen during one stress relaxation experiment. The original data were translated into stress or

load units by means of calibration software and processed mathematically and/or graphically by means of generally available data processing programs. The results described in this paper were obtained in stress relaxation mode in tension.

Materials

Besides the exploration of the effect of loading parameters on the structure of polymers and on their properties, we were interested to learn about the way in which the structure of the polymers, particularly crosslink density and network chain flexibility, affects their behavior in combined dynamic and static fields of stresses. Consequently, one of the major issues in this research became the choice of the investigated materials.

There are many ways to affect the crosslink density and flexibility of the resulting networks: changing the ratio between components,[32,33] varying curing conditions,[33,34] use of reactive diluents[35,36] or reacting epoxy and/or amine precursors with various functionalities.[35] The main drawback of the above mentioned techniques is that they lead to a network with a high concentration of structural defects (dangling chains, permanent entanglements and even trapped unreacted epoxy and/or amine molecules). Therefore, we opted for reacting one bifunctional epoxy resin (Epon Resin 825® from Shell Chemical Co.) with one diamine component (tetrafunctional) in proper stoichiometric ratio, while the variable factor was the structure of the crosslinking diamine.

In order to vary the crosslink density, the flexibility of the polymer structure, as well as the possibility of physical bond formation, the crosslinking agents were α,ω-aliphatic diamines (from Fluka A.G.) with various lengths of the aliphatic backbone:

$$NH_2—(CH_2)_n—NH_2$$

An additional reason for the choice of aliphatic diamines as crosslinking agents was the fact that they do not promote the etherification reaction,[30,31] as aromatic diamines do. The raw materials were investigated by infrared spectroscopy (IR) and found to be of adequate quality for our work without need of further purification. A concise characterization of the materials used in this study is provided in Table I. Since the most significant changes in the thermo-mechanical behavior of the networks are expected to take place while increasing the length of the aliphatic chain in the crosslinking agent up to 6 methylenic units,[29] the longest crosslinking agent investigated in this work was 1,6-hexamethylenediamine.

TABLE I
Molecular and equivalent weights of the amine (AEW) and of the epoxy (EEW) in the investigated materials

Component name	Polymer symbol	Molecular weight	AEW	EEW
Epon 825		350	—	175
$NH_2—(CH_2)_2—NH_2$	EE	60	15	—
$NH_2—(CH_2)_4—NH_2$	EB	88	22	—
$NH_2—(CH_2)_6—NH_2$	EH	116	29	—

Specimen Preparation and Characterization

The specimens were dumbbell shaped with a rectangular 4×4 mm cross section and a gauge length of approximately 22 mm. Ten identical specimens were obtained from each batch of material by casting the well-mixed and degassed prepolymer mixture into a specially designed mould. Additionally, cylindrical specimens with an external dumbbell shape were produced by use of a specially designed mould which allowed the control of their wall thickness. The main objective for making these specimens was examination of the uniformity effect of shear stresses on the experimental results; it is well known[61] that in cylindrical specimens a much more uniform field of shear stresses is induced in torsion than in specimens with a rectangular cross section.

One of the main requirements for specimens used for mechanical testing is that they will be free of bubbles and voids. The occurrence of these defects is usually a result of the presence of air embedded during the mixing stage and trapped inside the specimen due to the rapid increase of the viscosity while curing. Many methods for avoiding creation of bubbles in cast specimens are described in the literature; degassing each of the components before mixing[37,38] and/or after mixing[39,40] is widely used, but there are also authors[41,42] who consider that keeping the mixture at room temperature before curing is satisfactory for a good disposal of embedded air bubbles. In a previous study,[43] as well as in the preliminary stages of the present one, we found that all of the above techniques were not well suited to our materials because bubbles remained in the cured epoxy resin.[44] We solved the problem by building a special device which allowed us to perform all of the necessary operations (including casting) required for preparation of specimens in vacuum. The vacuum level was about 10 cm Hg and the prepolymer mixture was kept under vacuum for about 8 minutes; under these conditions no losses of crosslinking agents were recorded. Specific problems were encountered when 1,6-hexamethylenediamine (HDA) was used as a crosslinking agent since it is solid at room temperature, while the other crosslinking agents and Epon 825 are liquid. Therefore, in order to mix HDA with the epoxy resin, a preheating stage to about 60°C was necessary and the mould was preheated to the same temperature as the mixture in order to avoid solidification of the HDA before reaction. At that temperature, the reaction between the epoxy and amine groups proceeds at high speed so that the operational window is very narrow. As a result of these difficulties, the specimens based on HDA usually contained a small amount of bubbles in their upper part. Before subjecting the specimens to any test, these bubbles were removed by polishing the specimens on 320 grit sandpaper. The specimens were transparent to such a degree that measurement of birefringence by transmittance was possible. A regular curing cycle had three stages: 1 hour at 50°C, 2 hr at 100°C and finally 1 hour at 130°C. DSC and IR tests showed that by use of this schedule the resins were completely cured. A small absorption peak at 916 cm^{-1} could be observed on IR curves obtained from EE specimens after curing, whereas in the IR tests performed on EB and EH specimens, this peak was absent. The occurrence of the peak is interpreted as an indication that a small amount of free epoxy groups is still present in the EE specimen.[49] The reason for the uncompleted reaction of the epoxide groups in the

EE specimens seems to be related to the higher chain stiffness of the network obtained when 1,2-ethylenediamine was used for crosslinking.

The thermo-mechanical properties of cured specimens were determined by means of differential scanning calorimetry (DSC) with a Mettler TA-3000 instrument and a 983 DuPont DMA (at a heating rate of 10°C/min). Their specific weight was measured by use of the hydrostatic method. The crosslinking density, expressed as the average molecular weight of network chains between sites of crosslinking, M_c, was determined theoretically by application of the formula for stoichiometric mixtures of tetrafunctional diamines and bifunctional diepoxides:[56]

$$M_c = (M_A + 2M_E)/3 \quad (1)$$

where M_A and M_E are the molecular weights of the diamine and of the epoxy resin, respectively. The Gehman torsional method (ASTM 1053-85) was used to estimate the glass transition temperature of the polymers and to compute the experimental crosslinking densities based on the theory of rubber elasticity:[57]

$$G = \phi\rho RT/M_c \quad (2)$$

where the front factor ϕ was taken as unity,[37] ρ is the specific weight of the polymer measured at room temperature and R is the gas constant.

The mechanical properties in tension were determined at room temperature by use of a Zwick 1445 tensile tester with 1 mm/min crosshead speed. The main results of the above tests and calculations are shown in Table II.

TABLE II
Some thermo-mechanical characteristics of control samples

Material	Crosslink density (theoretical) (g/mole)	Crosslink density (exper.) (g/mole)	T_g (DSC)[a] (°C)	T_g (DMA)[b] (°C)	Thermal expans. coeff.[c] $(°C^{-1}) \times 10^5$	Young's modulus (MPa)	Density (g/cm^3)
EE	253	196	117	127	16.6	731 ± 22	1.194
EB	263	360	117	129	15.9		1.178
EH	272	361	103	123	19.4	544 ± 23	1.162

[a]determined at the inflection point;
[b]determined at the peak location on loss modulus *vs* T curve;
[c] in the glassy range, determined by linear expansion.

One of the possible causes of the discrepancy between the theoretical and experimental crosslinking densities may be found in the errors in modulus determination, especially in the rubbery region (due to manual operation of the Gehman apparatus). Another cause may be related to the competitive effects of crosslinking inefficiency (leading to trapped network chains) and of strong physical interactions between the polar sites (leading to the formation of physical crosslinks).

Experimental Procedure

After a regular curing cycle, followed by natural over-night cooling in the oven, the specimens appear almost black between crossed polarizers. The fact that the image

was not completely black means that some residual stresses are present and their origin is seemingly due to the curing process itself[45,46] or to the cooling procedure to room temperature.[47] These stresses were removed during the experiment by providing a stage of 20 minutes preheating of the specimens to a temperature higher than the T_g of the material, and slow cooling (at 0.5°C/min) to the temperature of the experiment.[48] Heating the specimens at $T_g + 30$°C was done at a high rate while the specimen was unconfined at its upper end, this to allow its free expansion; the upper grip was closed only at the end of the cooling stage. Attainment of the thermal equilibrium of the specimens was ensured by keeping them at the temperature of the experiment for at least 30 minutes before loading. The experiments lasted one hour and were followed by slow cooling to room temperature without discontinuing the flow of dry nitrogen.

RESULTS AND DISCUSSION

The typical shape of a stress relaxation curve obtained in the above described experimental regime is shown in Figure 2 in stress-time coordinates.

According to the procedure applied by Kubat and Rigdahl,[50] the data were plotted in a logarithmic time scale, instead of the often-used linear one, this revealing that most of the experimental points lie on a straight line (Fig. 3) whose equation is:

$$\sigma(t) = \sigma(0)_{K-R} - S\log(t) \tag{3}$$

where $\sigma(t)$ is the value of the measured tensile stress at any time, t, during the experiment (MPa). The values of the y-intercept ($\sigma(0)_{K-R}$) and of the slopes were

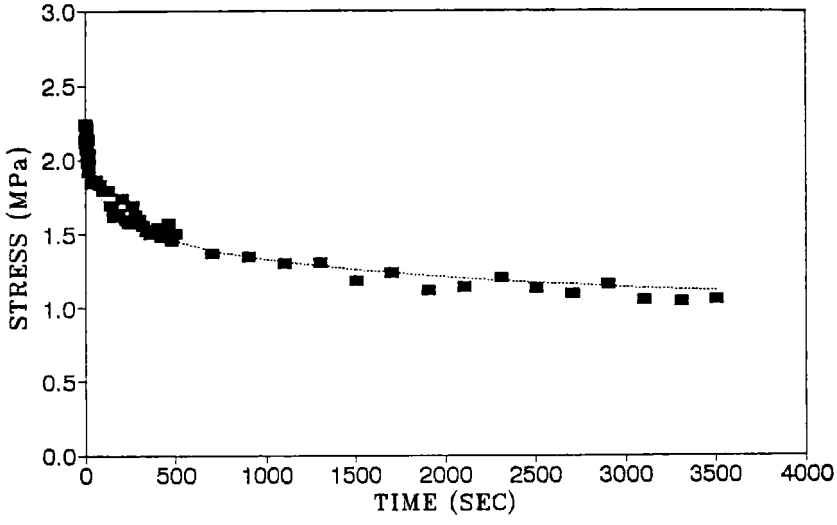

FIGURE 2 Typical stress relaxation curve, in coordinates σ-t, obtained in the glassy range at a tensile strain of 1%.

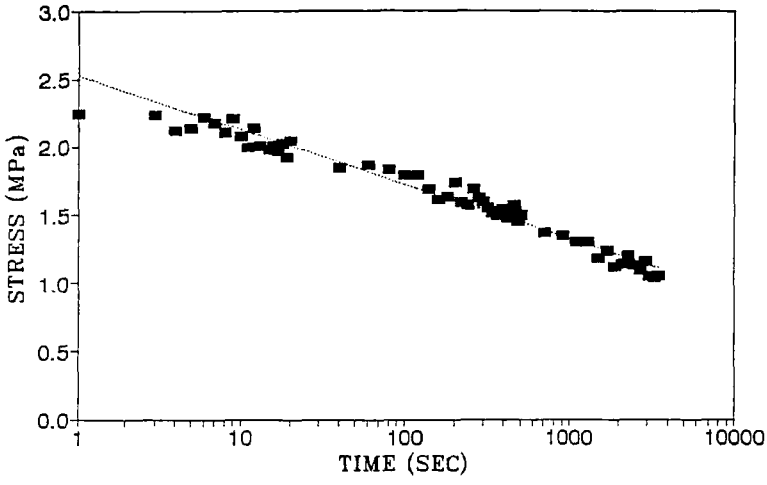

FIGURE 3 Same data as in Fig. 2 but in semilogarithmic representation: σ-log(t). The dotted line was obtained by linear regression.

computed by the least square linear regression from data collected during the experiment. The straining of the specimens requires usually about 1 second; therefore, in agreement with the factor-of-10 rule,[51,52] data from the first 10 seconds after straining are not included in the regression analysis. Usually, the correlation coefficient (R^2) is around 0.9. Lower R^2 were recorded at higher temperatures (above T_g) due to the relatively low signal-to-noise ratio of the instrument in this temperature range. In the following discussion, the stress relaxation rate was estimated by using the slope of the σ-log(t) line according to the equation:

$$SRR = (S/\sigma_0) \times 100 \tag{4}$$

where σ_0 is the initial stress (measured 1 second after the straining). The normalization procedure proved to be necessary, because S depends linearly on the magnitude of σ_0.[44]

The temperature at which the experiments were performed affects the relaxation times in a way strongly depending on the structure of the investigated polymers (Fig. 4).

Each point in Figure 4 is calculated as an average stress relaxation rate (computed as described above) from data collected in stress relaxation experiments performed on multiple specimens at some specific temperature. The error bars express two kinds of experimental errors: one of them originates in the noise of the measuring system and the other is connected with differences existing between different specimens. The first one emerged as the standard error of coefficients calculated by linear regression using data for one specimen, while the second is best described by the standard deviation of coefficients calculated for different specimens tested in the same conditions. The relatively high observed scatter of data in this work was expected, since it is a known problem when experimenting with epoxy resins;[9,53–55] that was the main reason for designing our apparatus so that it would be able to test five specimens simultaneously. Each one of the SRR-T curves is characterized by a

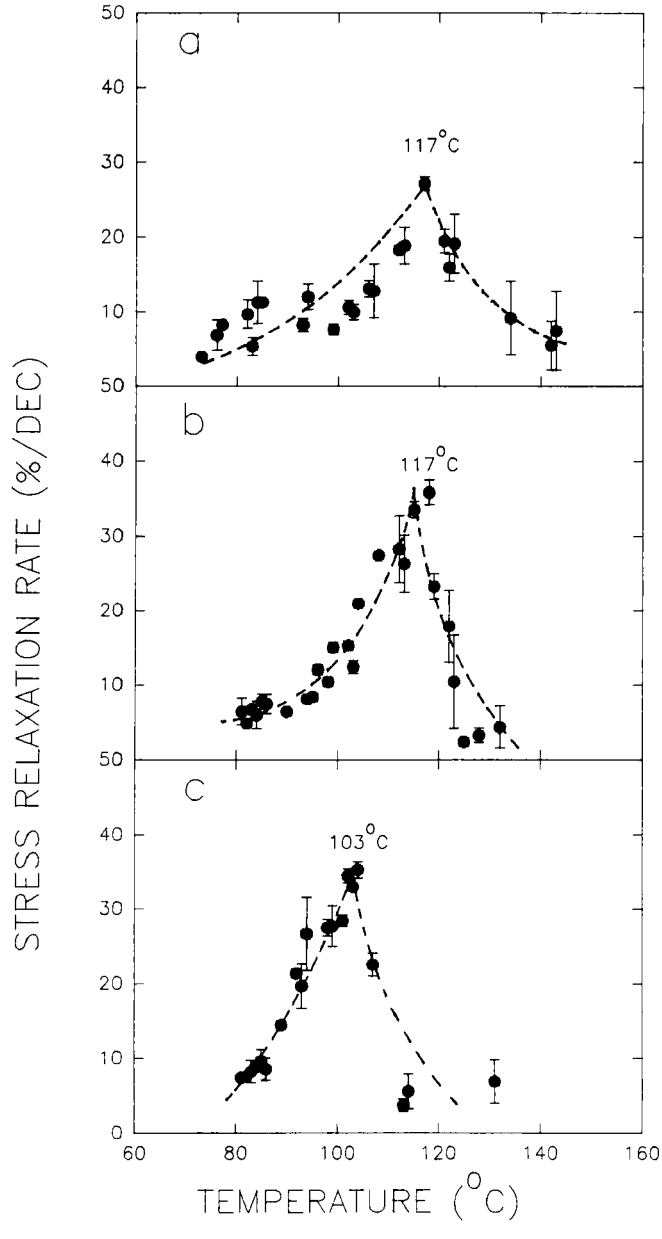

FIGURE 4 Effect of temperature on the stress relaxation rate of specimens based on the epoxy resin Epon 825® crosslinked with **a:** 1,2 Ethanediamine (EE), **b:** 1,4 Butanediamine (EB), and **c:** 1,6 Hexanediamine (EH).

maximum located at the T_g (inflection point), as determined by DSC and Gehman methods. The order of magnitude of the stress relaxation rates for all the investigated materials was the same in the glassy and rubbery regions. Based on molecular mobility considerations, we expected that, in the transition zone, the tensile stress relaxation of specimens subjected only to tensile stresses would be faster for the more flexible networks (EB and EH) than for the stiffer one (EE), which was indeed the case. The broadness of the glass transition zone is expressed by the width of the SRR-T curve; the more flexible the network, the narrower is the glass transition zone. This observation was confirmed also by DSC, DMA and Gehman tests,[44,58] and is supported by literature data.[29,32,36]

Experiments in which the tensile stress was supplemented by a static or dynamic torsional stress were designed in order to evaluate whether, and to what extent, the molecular mobility of the investigated resins was affected by the complex fields of stresses. The molecular mobility in the glassy and transition regions was estimated in terms of stress relaxation rate, computed as described above. Experiments performed in tension only served as points of reference.

Our expectations were based on free volume considerations: application of a torsional momentum on specimens confined at both ends should lead not only to torsional stresses but also to tensile stresses which result from a mechanism best described by the well-known Poynting effect,[59] Figure 5.

In the sub-T_g range, the Poisson's ratio, μ, is lower than 0.5 so that, consequently, the higher the tensile strain, the larger should be the dilatation effect:[60]

$$\Delta V/V_0 = \epsilon(1-2\mu) > 0 \tag{5}$$

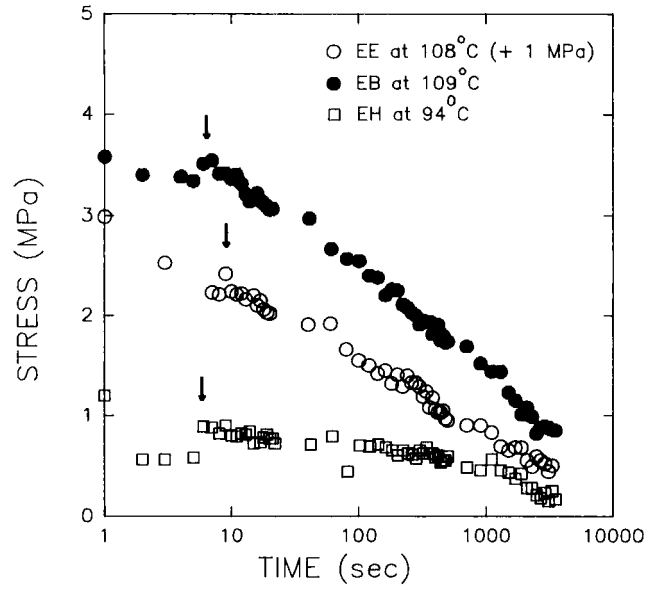

FIGURE 5 The Poynting effect as related to our experiments: an additional tensile stress was recorded (see arrows) when a torsional momentum was applied on tensioned specimens. Data concerning the EE specimen were shifted down by 1 MPa for the clarity of presentation.

Assuming that the additional volume obtained by straining the polymer in torsion will contribute to increase in the free volume fraction from f_o (for the polymer already strained in tension at 1%) to f, and using the WLF approach, one should expect a reduction of the relaxation times:[60]

$$f = f_o + \Delta V/V_o \tag{6}$$

$$\ln a_T = A(1/f - 1/f_r) \tag{7}$$

where f_r is the free volume fraction at some reference temperature and a_T is the relaxation time at some temperature, T, normalized to the relaxation time at the reference temperature. In other words, it was expected that the stress relaxation rates in tension for specimens subjected simultaneously to tension and torsion, at temperatures below T_g, will be higher than those recorded in experiments in which only tensile stresses were applied. In Figure 6 stress relaxation rates in tension are plotted against temperature: the graph shows that, within the limits of experimental error, the predictions based on the above model were correct in the case of EE specimens, but they were less met for the EB specimens and wrong for the most flexible polymer investigated in this work (EH). There were even cases in which the stress relaxation rate in tension for specimens subjected to tension and static torsion were smaller than those recorded for specimens subjected only to tensile stresses. Interestingly, the maximum of the SRR-T curve shifts to the left for the EE and EB specimens, a fact which may be interpreted as a decrease of the glass transition temperature. Similar phenomena of reduction of T_g upon straining have been widely reported in the literature.[6,7,17,60,62,63]

The above "dilatational" model,[60] when applied to combinations of tension and torsion,[44] may explain different related phenomena reported in the literature: Bergen *et al.*,[7] Baev and Malinin,[8] Onaran and Findley[12,13] and many others used similar combinations of static tensile and torsional loads on thermoplastic specimens confined at both ends, and recorded an increase in molecular mobility, expressed, usually, by larger creep rates.

However, the fact that predictions of this model are not fulfilled in the case of EH specimens leads us to the conclusion that perhaps another process is competing with the dilatation effect. This additional process, which leads to an increase in the relaxation times of the polymer, seems to be more significant when the flexibility of the network is larger, so that in the particular tension-static torsion loading conditions used in this work, it even overcomes the dilatation effects in the case of the most flexible structure investigated (Fig. 6). Such a process may be either of a chemical nature (continuation of crosslinking reactions during the stress relaxation experiment) or a physical one (physical aging, molecular orientation). In agreement with our previous data,[4,44,68] the process seems to be physical, since no continuation of crosslinking reactions could be detected. Similar results concerning a stiffening of the structure as a result of tension loading were reported recently by Guzman *et al.*;[17,64,65] they applied high tensile strains (up to 600%) to aliphatic and aromatic polyester networks and recorded increased storage moduli when the tensile strain was increased above certain values. In their work, the tensile strains were applied while the specimens were in their rubbery state and the dynamic mechanical analysis was performed in their glassy state, after quenching the samples from above T_g.

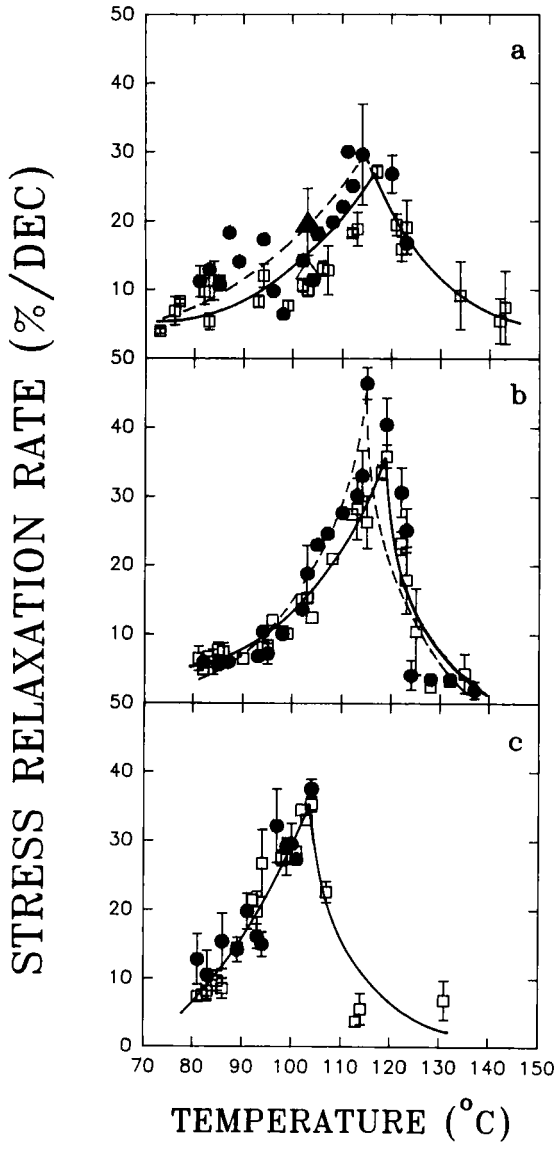

FIGURE 6 The effect of temperature and specimen composition on the tensile stress relaxation rate, in tension (hollow symbols) and combined tension and static torsion (filled symbols). Triangles—cylindrical specimens. **a:** EE, **b:** EB, **c:** EH specimens.

Differences in the experimental approach (in our work the specimens were strained up to only 1% in the glassy state) and in the packing efficiency of the investigated networks (our networks are much denser than theirs) make the comparison between results quite difficult. In any event, our results, like the reports of Guzman *et al.*, point to the same phenomenon; straining the polymers in the glassy state (where Poisson ratio $\mu<0.5$) does not lead always to loosening the structure (dilatation effect), but might induce a reduction of the molecular mobility, depending on the straining conditions and crosslink density. In other words, it seems that the behavior of our crosslinked epoxy resins, in complex fields of static tension and torsion, is governed by a balance between two competitive processes, one leading to a decrease, and the other to an increase, respectively, of the relaxation times.[70] This conclusion is supported by recent results of Song and Roe[71] and of Chow[72] who showed that free volume itself is not enough to characterize the glassy state of polymers; an additional ordering parameter is needed and this is the molecular packing.

When dynamic torsional stresses were superimposed on tensile stresses, SRR-T curves shown in Figure 7 were obtained.

The increase of tensile stress relaxation rates (in the glassy state) in these conditions was much more significant than that recorded in combined static torsion-tension experiments, both being compared with the stress relaxation rates encountered when only tension loads were applied. A comparable phenomenon was reported by Struik:[66] the creep rate was much larger when intermittent, rather than continuous, loading was used. Similarly, a substantial decrease in the viscosity of polymer solutions was reported as a result of subjecting them to combined steady and oscillatory shear.[18,67] In both cases, the material structure becomes less efficiently packed than in the reference loading state either by halting the physical aging process in cyclic loading[67] or by destruction of the supermolecular structure of the polymeric solution.[18]

Subjecting EB and EH specimens to complex dynamic and static loading led to an even more pronounced trend of deviation of the results from the simple dilatation model (Fig. 8 and Fig. 9, respectively).

At the lowest frequency of torsional oscillations, the tensile stress relaxation rates of EB specimens in the glassy region were still a little higher in combined loading than in simple tension (Fig. 8a), but for EH specimens (Fig. 9a) superposition of dynamic stresses on the static one led to an obvious decrease of the stress relaxation rate. An increase in the frequency of torsional oscillation seems to contribute to further decrease of the tensile stress relaxation rates, both for EB and EH specimens. It is worthwhile mentioning that a similar, but much more moderate trend, can be observed with EE specimens: at the highest torsional frequency ($\nu = 16.6$ Hz, Fig. 7c), some stress relaxation rates measured in these combined loading conditions were smaller than those encountered in tension only. Based on the assumption expressed earlier that an additional process competes with the dilatation effect, we may conclude that a dynamic torsional stress is much more effective in increasing the relaxation times than a torsional static stress, when either one of them is imposed on a tensile static stress.

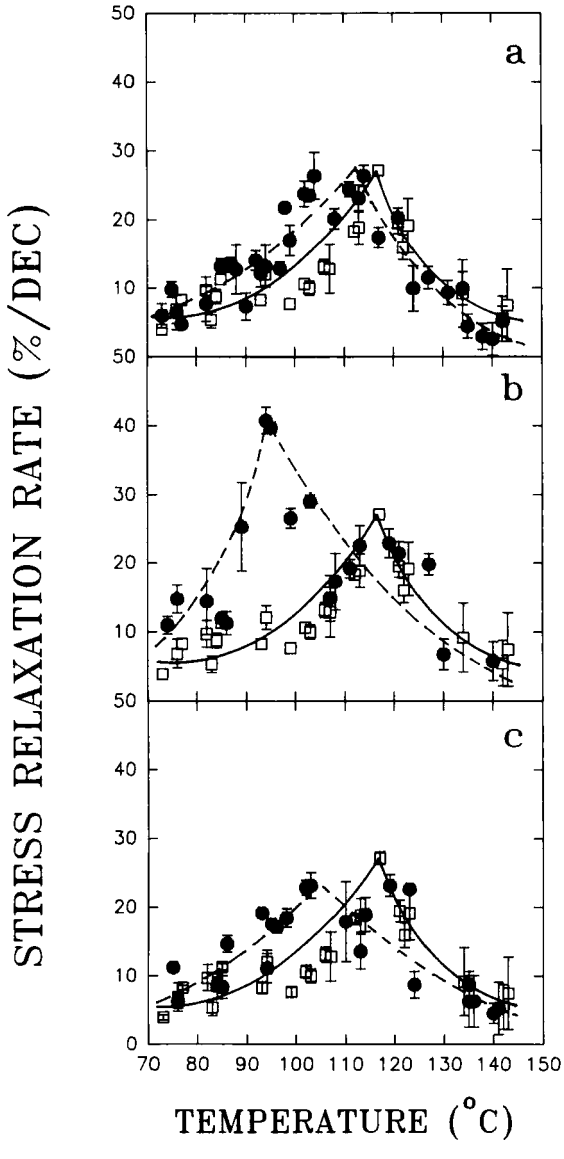

FIGURE 7 Effect of temperatue and frequency of torsional oscillations superimposed on the tensile strain on stress relaxation rate in tension of EE specimens. **a:** υ-0.83 Hz; **b:** $\upsilon = 8.5$ Hz; **c:** $\upsilon = 16.6$ Hz. Triangular symbols—cylindrical specimens.

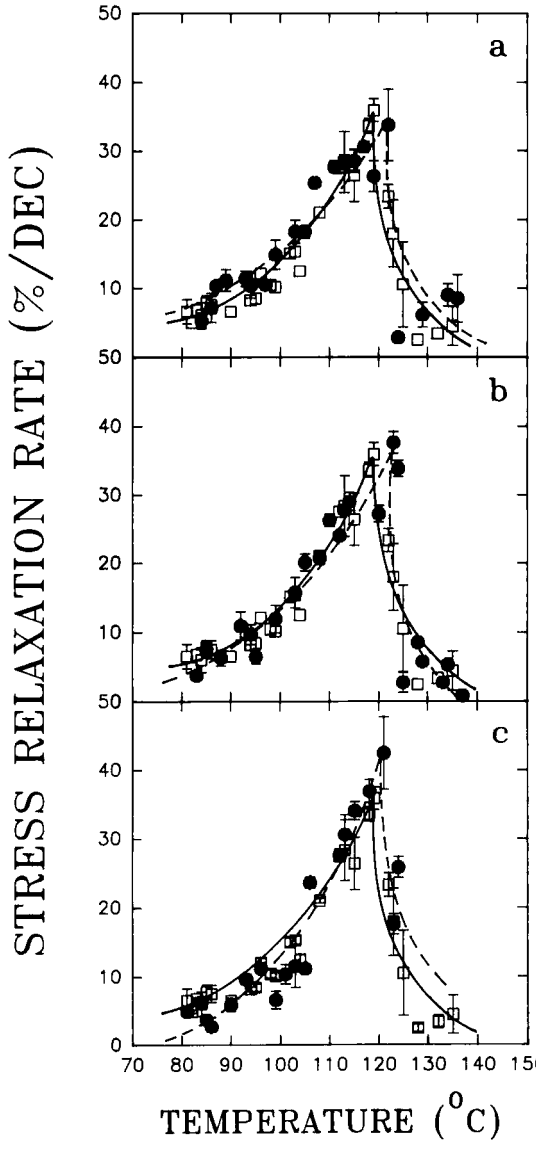

FIGURE 8 Effect of temperature and frequency of torsional oscillations superimposed on the tensile strain on stress relaxation rate in tension of EB specimens. **a:** $\upsilon = 0.83$ Hz; **b:** $\upsilon = 8.5$ Hz; **c:** $\upsilon = 16.6$ Hz.

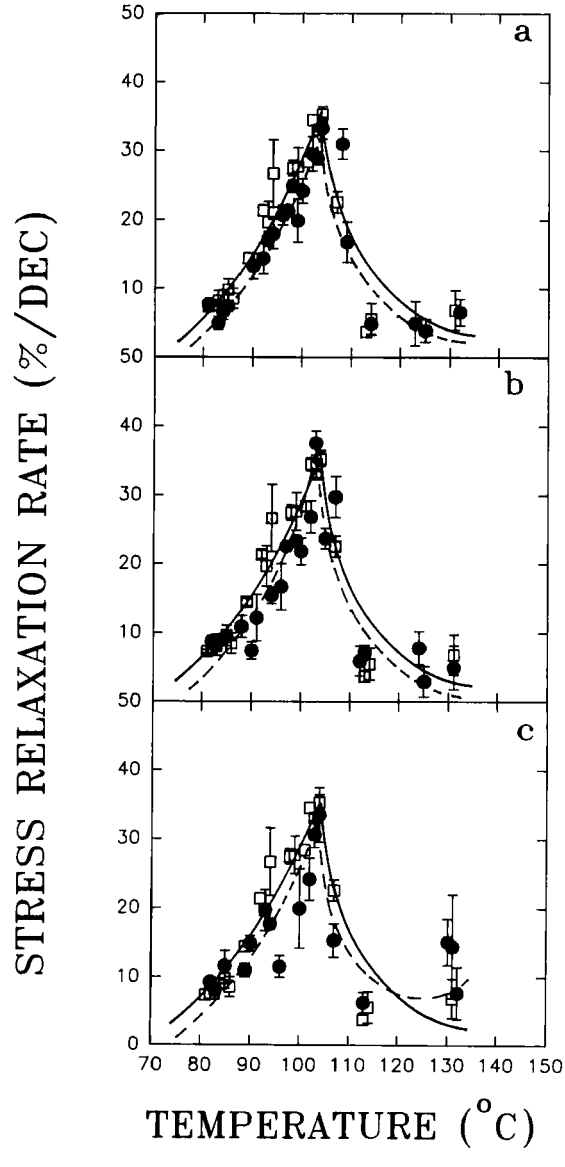

FIGURE 9 Efect of temperature and frequency of torsional oscillations superimposed on the tensile strain on stress relaxation rate in tension of EH specimens. **a:** $\upsilon = 0.83$ Hz; **b:** $\upsilon = 8.5$ Hz; **c:** $\upsilon = 16.6$ Hz.

CONCLUSIONS

The rheological behavior of the investigated resins seems to be governed by a balance between two competitive processes. One of them leads to a decrease in the

relaxation times by a mechanism involving, supposedly, an increase in the free volume fraction due to strain dilatation. The other process acts to increase the relaxation times (as expressed by reduced stress relaxation rates) through a mechanism not involving continuation of crosslinking reactions.[44] The picture emerging from the reported results is that, in its glassy state, the most rigid investigated polymer system becomes more flexible when subjected to complex fields of stresses. Apparently, the increase of molecular mobility due to strain dilatation is larger for this polymer than the decrease in molecular mobility induced by the competitive process. On the other hand, the more flexible resins show a tendency to become more rigid (reduced stress relaxation rates) under combined dynamic and static stresses as a result of the fact that, in their case, the effect of strain dilatation is smaller than the effect of the competitive process. The viscoelastic behavior of the investigated model epoxy resins in complex fields of dynamic and static stresses cannot be predicted based on a linear combination of the effects of the component stresses, taken separately.

In other words, the competitive process seems to be dependent not only on the state of stresses acting on the specimen but also, and to a large extent, on the flexibility of the network chains; the effect of superimposed dynamic and static stresses on the rheology of the investigated resins is highly non-linear. We suggest that, due to the relatively high molecular mobility of the more flexible networks in their glassy state, the interaction between the polar sites is more enhanced than in the more rigid ones. Moreover, subjecting flexible networks to stresses may result in local orientation of network chains which may enhance even further the interaction between the polar groups. Hence, as a result of this particular experimental combination between resin flexibility and complexity of applied stresses, we expect an overall better packing efficiency of the resin which would express itself by increasing the relaxation times.

This conclusion may affect the way in which we think about the behavior of composites (based on thermoset materials) in complex fields of dynamic and static stresses. The interphase and the bulk polymer in these composites may have the same chemical structure, but their crosslink density might be different. Particularly, the crosslinking density of the interphase could be lower than that of the bulk, mainly because of steric hindrances caused by the proximity of the solid substrate (filler) and/or selective adsorption of functional groups by that substrate. Ultrasonic Rayleigh wave measurements of elastic modulus of epoxy adhesives close to a metallic substrate, performed by Knollman,[73] support this hypothesis. An additional cause for the lower crosslink density of the interphase may be related to the fact, recently reported,[69] that the viscosity of polymeric liquids, when measured close to a solid substrate, is several orders of magnitude higher than that measured in the mass of the same liquids. Therefore, the crosslinking reactions taking place close to the liquid-filler boundary could be significantly slower than those in the main mass of the liquid resin, so that at the end of the curing process of the composite, the polymeric interphase might be, in fact, incompletely cured. In view of the above results, it is suggested that polymeric interphases in thermoset-based composites, while originally perhaps softer than the bulk, may become more and more hard when subjected to complex fields of dynamic and static stresses.

References

1. S. Bron and D. Katz, Proc. of 4th Israel Materials Engineering Conference, Beer-Sheva, 1988.
2. D. Katz and S. Bron, *Makromol. Chemie, Macromol. Symp.* **23,** 381 (1989).
3. D. Katz and S. Bron, *J. Mater. Sci.* **26,** 4733 (1991).
4. S. Bron and D. Katz, *J. Adhesion,* 1993 in press.
5. R. S. Duran and G. B. McKenna, *J. Rheology* **34,** 813 (1990).
6. S. S. Sternstein and T. C. Ho, *J. Appl. Phys.* **43,** 4370 (1972).
7. J. T. Bergen, D. C. Messersmith and R. S. Rivlin, *J. Appl. Polym. Sci.* **3,** 153 (1960).
8. L. V. Baev and N. I. Malinin, *Mekh. Polim.* **2,** 671 (1966).
9. K. Ikegami, M. Kajiyama, S. Kamiko and E. Shiratori, *J. Adhesion* **10,** 25 (1979).
10. T. Nishitani, *J. Mater. Sci.* **12,** 1185 (1977).
11. E. S. Umanskii, B. Y. Lyashenko, Y. K. Zhakov and R. A. Veselovskii, *Ind. Lab.* **43,** 1725 (1977).
12. K. Onaran and W. N. Findley, *Trans. Soc. Rheol.* **9:2,** 299 (1965).
13. W. N. Findley and K. Onaran, *Trans. Soc. Rheol.* **12:2,** 217 (1968).
14. Z. H. Stachurski and I. M. Ward, *J. Polym. Sci., Part A-2* **6,** 1083 (1968).
15. J. M. Crissman and L. J. Zapas, *J. Appl. Phys.* **48,** 4049 (1977).
16. T. Ricco and T. L. Smith., *Polymer* **26,** 1979 (1985).
17. R. Diaz-Calleja, E. Riande and J. Guzman, *Polymer* **28,** 2190 (1987).
18. A. I. Isayev, V. A. Zolotarev and G. V. Vinogradov, *Rheol. Acta* **14,** 145 (1975).
19. R. I. Tanner, *Trans. Soc. Rheol.* **12,** 155 (1968).
20. K. Osaki, M. Tamura, M. Kurata and T. Kotaka, *J. Phys. Chem.* **69,** 4183 (1965).
21. H. C. Booij, *Rheol. Acta* **5,** 222 (1966).
22. T. Kotaka and K. Osaki, *J. Polym. Sci., Part C* **15,** 453 (1966).
23. J. L. Sullivan and V. C. Demery, *J. Polym. Sci., Polym. Phys. Ed.* **20,** 2083 (1982).
24. J. L. Sullivan, *J. Appl. Polym. Sci.* **28,** 1993 (1983).
25. S. Bron and D. Katz, Proc. of the 5th Israel Materials Engineering Conf., December 1990, Haifa, Israel.
26. S. Bron and D. Katz, Proc. of SAMPE Tech. Conf., Maastricht—The Netherlands, May 1991.
27. S. Bron and D. Katz, Proc. of SAMPE Tech. Conf., New York—USA, October 1991.
28. S. S. Sternstein, in *Polymer Characterization,* C. D. Craver, Ed., ACS Series, **203,** 123 (1983).
29. T. K. Kwei, *J. Polym. Sci., Part A-2* **4,** 943 (1966).
30. C. C. Riccardi and R. J. J. Williams, *J. Appl. Polym. Sci.* **32,** 3445 (1986).
31. R. Lovell and A. H. Windle, *Polymer* **31,** 593 (1990).
32. T. Murayama and J. P. Bell, *J. Polym. Sci., Part A-2* **8,** 437 (1970).
33. V. B. Gupta, L. T. Drzal, G.Y-C. Lee and M. J. Rich, *Polym. Eng. Sci.* **25,** 812 (1985).
34. Y. Leterrier and C. G'Sell, *J. Mater. Sci.* **23,** 4209 (1988).
35. V. Bellenger, E. Morel and J. Verdu, *J. Mater. Sci.* **23,** 4244 (1988).
36. S. Qureshi, J. A. Manson, J. C. Michael, R. W. Hertzberg and L. H. Sperling, in *Characterization of Highly Crosslinked Polymers,* S. S. Labana and R. A. Dickie, Eds., (Am. Chem. Soc. Washington, DC, 1984), p. 109.
37. J. D. LeMay, PhD Dissertation, University of Akron, Akron, Ohio, USA (1985).
38. W. Wu and B. L. Bauer, *Polymer* **27,** 169 (1986).
39. H. S. Chu and J. C. Seferis, *Polym. Comp.* **5,** 124 (1984).
40. A. Lee and G. B. McKenna, *Polymer* **31,** 423 (1990).
41. R. J. Crowson and R. G. C. Arridge, *J. Mater. Sci.* **12,** 2154 (1977).
42. N. G. McCrum and G. A. Pogany, *J. Macromol. Sci., Phys.* **B4,** 109 (1970).
43. S. Bron, M.S. Thesis, Technion—Israel Institute of Technology, Haifa, Israel, 1988.
44. S. Bron, PhD Thesis, Technion—Israel Institute of Technology, Haifa, Israel, 1992.
45. A. K. Srivastava and J. R. White, *J. Appl. Polym. Sci.* **29,** 2155 (1984).
46. T. Igarashi, S. Kondo and M. Kurokawa, *Polymer* **20,** 301 (1979).
47. M. Shimbo, M. Ochi and Y. Shigeta, *J. Appl. Polym. Sci.* **26,** 2265 (1981).
48. A. Siegmann, A. Buchman and S. Kenig, *Polym. Eng. Sci.* **22,** 40 (1982).
49. O. Delatycki, J. C. Shaw and J. G. Williams, *J. Polym. Sci., Part A-2* **7,** 753 (1969).
50. J. Kubat and M. Rigdahl, in *Failure of Plastics,* W. Brostow and R. D. Corneliussen, Eds. (Hanser Publ., Munchen, 1986), p. 60.
51. T. Ho, J. Mijovic and C. Lee, *Polymer* **32,** 619 (1991).
52. K. S. C. Lin and J. J. Aklonis, *J. Appl. Phys.* **51,** 5125 (1980).
53. G. C. Knollman, *Int. J. Adh. Adh.* **5,** 137 (1985).
54. W. J. Cantwell, A. C. Roulin-Moloney and T. Kaiser, *J. Mater. Sci.* **23,** 1615 (1988).
55. D. H. Kaelble, *J. Appl. Polym. Sci.* **9,** 1213 (1965).

56. A. C. Grillet, J. Galy, J-F. Gerard and J-P. Pascault, *Polymer* **32,** 1885 (1991).
57. J. D. Ferry, *Viscoelastic Properties of Polymers* (John Wiley and Sons, New York, 1970).
58. S. Bron, unpublished results.
59. J. H. Poynting, *Proc. Roy. Soc. (London)* **A86,** 534 (1912).
60. S. Matsuoka, C. J. Aloisio and H. E. Bair, *J. Appl. Phys.* **44,** 4265 (1973).
61. E. P. Popov, *Mechanics of Materials,* 2nd Ed. (Prentice/Hall Int., Inc., New Jersey, 1978), p. 78.
62. T. S. Chow, *Polym. Eng. Sci.* **24,** 1079 (1984).
63. A. I. Isayev and D. Katz, *Intern. J. Polym. Mat.* **8,** 25 (1980).
64. R. Diaz-Calleja, E. Riande and J. Guzman, *J. Polym. Sci., Polym. Phys. Ed.* **24,** 337 (1986).
65. E. Riande, J. Guzman and M. A. Llorente, *J. Polym. Sci., Polym. Phys. Ed.* **21,** 2473 (1983).
66. L. C. E. Struik, *Physical Aging in Amorphous Polymers and other Materials* (Elsevier, Amsterdam, 1978).
67. R. I. Tanner and J. M. Simmons, *Chem. Eng. Sci.* **22,** 1803 (1967).
68. Y. S. Lipatov and L. M. Sergeeva, *Adsorption of Polymers* (John Wiley and Sons, New York, 1972), p. 142.
69. J. van Alsten and S. Granick, *Macromolecules* **23,** 4856 (1990).
70. D. Katz, "Microphase Separation in Densely Crosslinked Polymers," in *Polymer NDE,* K. H. G. Ashbee, Ed. (Technomic Publ. Co. Inc., Lancaster, PA, 1986), p. 19.
71. H.-H. Song and R.-J. Roe, *Macromolecules* **20,** 2723 (1987).
72. T. S. Chow, *Macromolecules* **22,** 701 (1989).
73. G. C. Knollman and J. J. Hartog, *J. Appl. Phys.* **53,** 1516 (1982).